CHAPTER VI

ROOM TEMPERATURE WEAK FERROMAGNETISM OF Mn DOPED CuI FILMS

6.1 Introduction

The field of diluted magnetic semiconductors (DMSs) have gained attraction of the researchers due to their exclusive properties and their increasing demand in the areas of device physics such as optoelectronic and spintronics (J. Zhang et.al, 2017). DMSs are actually semiconductors that are non-magnetic in nature which exhibit magnetism when doped with some amount of magnetic impurities, usually transition metals. This strategy of ferromagnetic semiconductor uses the charge of the electron as well as the spin of the electron which is an intrinsic nature of its own. The intrinsic spin of the electron has much more advantage than that of the charge of the electron in terms of their manipulation with external magnetic field and long coherence which normally cannot get affected on account of collisions with defects, impurity scattering etc., Hence this technology get along with conventional semiconductor technology with high spin polarisation an advantage of spintronics (K.M. Yuet.al 2003, J. Tang et.al 2015). Varying the concentration of the dopant (transition metals) with semiconductors in turn changes the lattice parameters, energy gap, magnetic and optical properties of DMS materials.

Copper(I) iodide nanoparticles being p-type semiconductors are new functional materials widely used in chemical fibres, polymers, catalyst and semiconductors (Hong Tao Lia, 2007). They exhibit remarkable properties of electrical conductivity and optical transparency in the visible region with the optical bandgap of about 2.3 – 3 eV (S. Badyopadhyaya et.al, 2000). CuI is white in colour in its pure form and brown or tan in impure form. Copper iodide exists in three crystalline phases α, β and γ. CuI has cubic rock salt like structure in its α-phase and the presence of copper ions makes it conducting in nature

rather than the iodine counterpart. CuI is well known to exhibit the superionic behaviour in the high temperature, where the mobile Cu ions migrate between the sites in the sub-lattice of immobile iodine ions (J.B. Boyce et.al, 1981). The conductivity approaches 0.1 $\Omega^{-1}cm^{-1}$ in γ - phase is slightly higher in α-phase and in β phase it reaches higher value 1 $\Omega^{-1}cm^{-1}$ but the γ-phase conductivity depends on the presence of iodine in stoichiometric excess. The β-phase of CuI is hexagonal in structure and exhibits ionic conductivity, whereas the γ-phase of CuI exists in cubic zinc blende like structure which shows p-type semiconducting behaviour. These phases appear to change with temperature and it has been reported that CuI exists at its γ-phase up to 350º C, above which it turns to the α-phase at 392º C (Ishak Afşin Kariper, 2016). Nano-sized CuI has enormous applications in varying fields like catalysis, pharmaceuticals and electronics. It exhibits a property of ultrafast scintillation and its decay time at room temperature is found to be 90 ps, and hence it is considered to be one form of inorganic scintillation crystal material (P. Gao et.al, 2009).

A variation in the optical as well as electronic properties of semiconductor nanoparticles can be brought out by doping. The doped nanoparticles are of great importance in the field of nanotechnology due to their significant applications in the fields of electronics, optics, photonics, sensors and medicine. Manganese (Mn) a transition metal is a magnetic material that favourably exhibits ferromagnetism and antiferromagnetism when doped (C. E. Arrondo et.al, 2014). Materials that exhibit the properties of soft ferromagnetism or ferrimagnetism possess the properties of high permeability, high saturation induction and low coercive forces. Also even with weak magnetic field magnetisation is perceived or observed change in magnetization is possible using soft ferromagnetic materials (G. Zamiri et.al 2014). Also, the doping of a magnetic material like Mn, can bring about desirable change in the magnetic properties of the compound (N. Spaldin, 2003). Hence in our present work, we

prepared Mn doped CuI nanoparticles to understand its influence in the magnetic behaviour of CuI.

6. 2 Experimental

6.2.1 Materials

The chemicals used in the present work were of analytical grade, purchased from commercial sources and used as such. Copper (II) sulphate pentahydrate ($CuSO_4.5H_2O$) was purchased from Merck and sodium thiosulphate ($Na_2S_2O_3$) from HIMEDIA. Potassium iodide (KI) and manganese (II) chloride tetrahydrate ($MnCl_2.4H_2O$) (Loba Chemie) were purchased and used as such. Further all the experiments were carried out in deionised water.

6.2.2 Characterisation

The X-ray diffractions (XRD) of un-doped and Mn-doped CuI films were obtained on PANalytical X'Pert PRO powder X-ray Diffractometer, at a scanning range of $10–100^0$ with CuKα radiation of wavelength of λ =1.5406 Å. The UV-DRS spectra of the films were obtained by Agilent CARY 500 UV-VIS-NIR spectrophotometer at wavelength range of 300–1100 nm. The photoluminescence spectra of the films were recorded on SHIMADZU RF-6000 spectrofluorophotometer. The morphological studies were examined using Atomic Force Microscope Agilent 5100. The VSM studies were obtained on Cryogenic Vibrating Sample Magnetometer model 7407, Lakeshore.

6.2.3 Copper iodide and Mn doped copper iodide films preparations

The films of CuI were deposited in accordance with SILAR method (R. N. Bulakhe et.al, 2013) on prepared glass substrates. The glass surfaces were modified by employing wet and dry chemical cleaning methods prior to the deposition of films so as to improve the adhesive bonding between the glass surface and films. Substrates were washed with methanol and deionised water successively and dried at 120^0C. The substrates were first immersed in a solution containing 0.1 M $CuSO_4.5H_2O$, which was used as the cationic percursor and 0.1 M

$Na_2S_2O_3$ for 40 seconds. $Na_2S_2O_3$ play the role of both reducing and complexing agent and reduces Cu^{2+} to Cu^{+}. Finally the substrates were immersed in a solution of 0.025 M KI for another 40 seconds. The substrates were then rinsed with deionised water to remove the loosely held ions and dried the substrates at 60^0C for 4 hours and stored air tight.

The manganese doped CuI films with two different concentrations of manganese were deposited on the glass substrates. $CuSO_4.5H_2O$ and $MnCl_2.4H_2O$ were dissolved in 50 mL of deionised water. The concentration for $CuSO_4.5H_2O$ was 0.2 M and the concentrations of $MnCl_2.4H_2O$ were 0.01 M (5 mol% doping) and 0.02 M (10 mol% doping) respectively. The resultant mixtures were then subjected to stirring at room temperature for 1 h to obtain homogeneity. The glass substrates were cleaned with methanol for 15 minutes rinsed using deionized water and then dried in hot air oven prior to the deposition of the films. The CuI films and Mn doped CuI films were prepared without and with including $MnCl_2.4H_2O$ in the above mentioned procedure. The doped films were then dried for a period of 2 hours at 60^0C in a hot air oven.

6.3 Results and Discussion

6.3.1 Structural analysis

The crystal structure as well as phase purity of the as-synthesised CuI and Mn-doped CuI films were analysed using power X-ray diffractogram (Fig 6.1) which was recorded at room temperature with 2θ in the range 20 – 80°. All the peaks obtained in the XRD could be indexed exactly to the zinc blende phase of CuI which is in accordance with the reported standards (JCPDS No. 76-0207) in the literature and further no additional peaks were found in pristine or doped samples indicating that the films were phase pure. The peaks appear at 2θ values 25, 29, 42, 49, 52, 61, 67, 69 and 77 could be ascribed to (111), (200), (220), (311), (222), (400), (331), (420) and (422) hkl planes of γ-CuI respectively. All the CuI and Mn-doped CuI film samples were found to be oriented preferentially along (111) direction which

is evident from the diffraction patterns. The XRD patterns reveals slight shift in peaks position in Mn-doped CuI films towards higher angles, indicating a minor distortion in the symmetry arising due to the defects and vacancies created in the system (V. Thampi et.al, 2015). The crystallite size (D) of the films were calculated using Debye-Scherrer's formula

$$D = 0.9 \lambda / \beta \cos \theta$$

where β is the full width at half maximum (FWHM) in the peaks, θ is the angle of diffraction, λ the wavelength of the X-ray used (1.541 Å). The calculated value of crystallite size was found to be 36, 44 & 36 nm for the un-doped and Mn doped CuI films. The average crystallite size was found to increase on doping and then decreases for 10 mol% doping which could be due to high mobility along with low activation energy and small radius of the Mn ions. Since the activation energy is low, these ions can easily transfer from trap sites to nucleation sites during the process of crystal growth which in turn leads to larger crystallite size (P. Chand et.al 2014, W. Gao et.al 2010, J.S Shaikh et.al 2011).

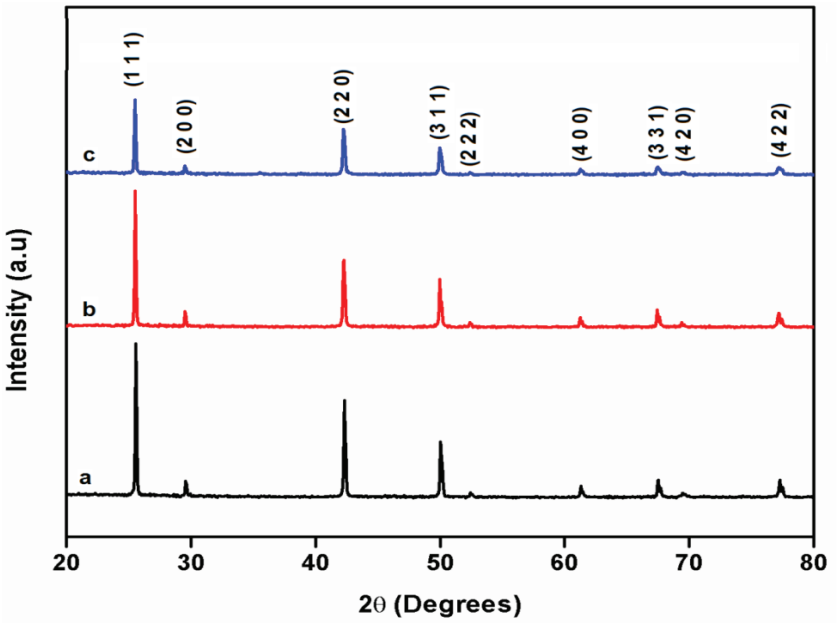

Fig 6.1 X-ray diffractogram of (a) CuI film (b) 5 mol% Mn-doped CuI (c) 10 mol% Mn-doped CuI

6.3.2 Optical studies

The optical behaviour of the un-doped and doped CuI films were studied using UV-visible absorbance spectrum recorded in the wavelength range of 200-900 nm. The transmittance spectra of CuI and Mn doped CuI films are displayed in Fig.6.2a revealing the transparency of all the samples in the visible region. The average transmittance for CuI and Mn doped CuI films with a Mn concentration of 5 mol% and 10 mol% are observed to be 50, 26 and 25% in the visible range, respectively. This decrease in optical transmittance is ascribed to the loss of incident photon caused by the defects which arises as a result of doping and scattering of photon at the grain boundaries (F. Ozutok et.al, 2012). Optical bandgap energies of the prepared films were obtained from Tauc relation given by

$$\alpha h\nu = A'\left(h\nu - E_g\right)^n$$

where α =2.303A/t is called the coefficient of absorption, A being the absorbance and t, the wave path length equal to the cuvette thickness, A′ is called proportionality constant, E_g being the bandgap energy, hν is the energy of photon and for direct transition the value of n is found to be 1/2. From the Tauc plots (Fig. 6.2b), it can be observed that the bandgap of undoped CuI films is 2.9 eV and that of 5 mol% and 10 mol% Mn doped CuI films are 2.77 and 2.76 eV respectively. The decrease in bandgap with increasing concentration of Mn dopant may be attributed to the increase in particle size.

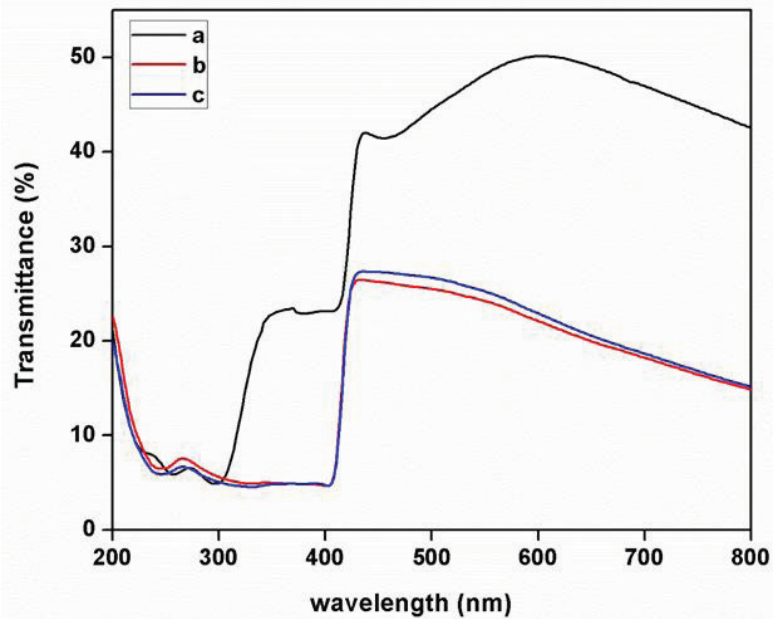

Fig 6.2a Transmittance spectra of (a) CuI (b)5 mol% Mn-doped CuI (c) 10 mol% Mn-doped CuI films

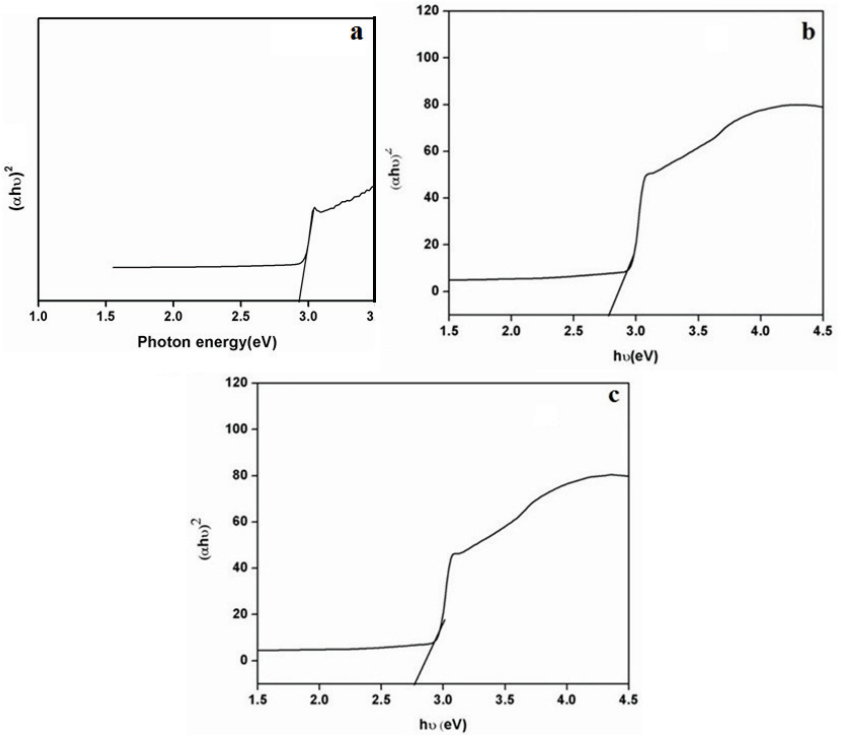

Fig 6.2b Tauc plots showing the variation of $(\alpha h\nu)^2$ with photon energy for (a) CuI (b) 5 mol% Mn-doped CuI (c) 10 mol% Mn-doped CuI films

The optical absorbance spectra of CuI and Mn doped CuI films are displayed in Fig. 6.2c. The absorption peak appears at 297 nm for the un-doped CuI sample while on doping Mn, the optical absorption edge is slightly shifted towards longer wavelength at 331 nm. The possible reason for this red shift is attributed to the decrease in band gap of Mn doped CuI films (S.A. Ahmed, 2017).

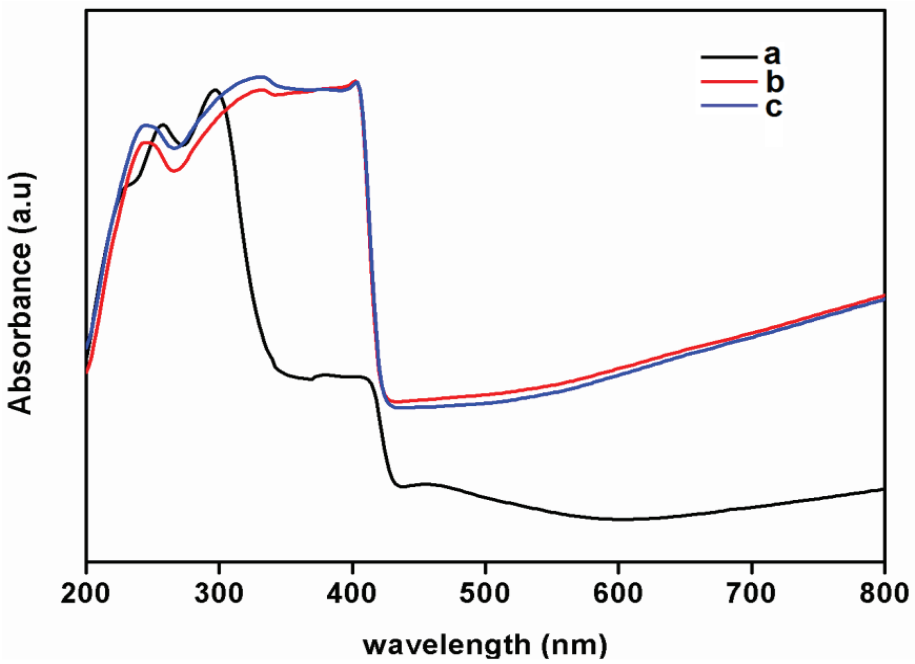

Fig 6.2c Absorbance spectra of (a) CuI (b) 5 mol% Mn-doped CuI (c) 10 mol% Mn-doped CuI films

6.3.3 Photoluminescence

Photoluminescence is one of the important studies used in identifying the quality of films (K.D.A. Kumar et.al 2018, V. Ganesh et.al 2017). It is also used to identify the electron-hole surface progressions and impurities in semiconductor materials and also specific defects for radiative transitions (M. Anpo et.al, 1989). From the literature, it is inferred that the emission wavelength is influenced by the size as well as the morphology of the particle, dopant concentration and excitation wavelength (A. Ahmed et.al, 2011). Therefore, the effect of Mn doping on the photoluminescence property of the synthesized CuI nanostructures is studied by recording the PL spectra of undoped and Mn doped CuI films (Fig.6.3) with an excitation wavelength of 320 nm. It is observed that the emission spectrum of undoped and doped CuI films possess a prominent band at 418 nm in the blue region. Comparing the PL spectra of the doped and undoped film, no new emission peaks were observed except for a small change in the emission intensity, followed by a bathochromic shift of the peaks on doping with Mn (M. Shkir et.al, 2018).

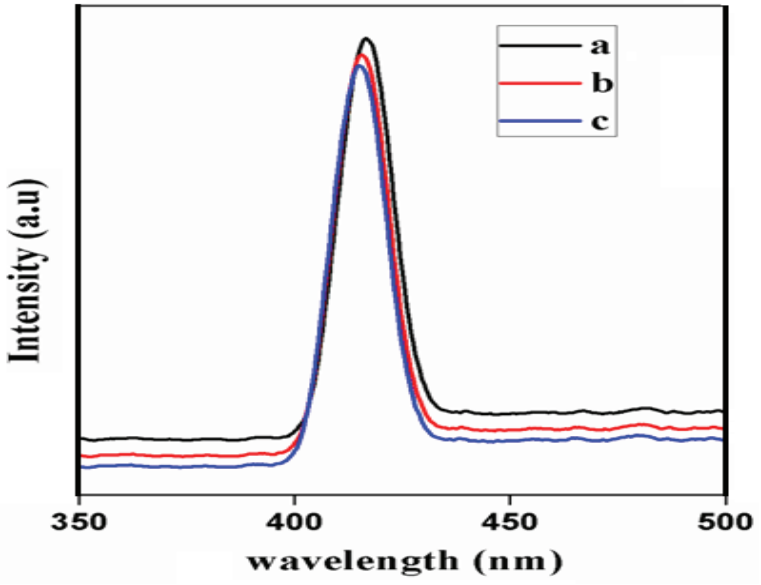

Fig 6.3 Photoluminescence spectra of (a) CuI (b) 5 mol% Mn-doped CuI (c) 10 mol% Mn-doped CuIfilms

6.3.4 Surface Analysis

The AFM measurements could provide information regarding the surface morphology of the films and this capability might be used to investigate the nature of the deposited films like the surface roughness and particle size. A careful analysis of roughness can yield information regarding the kind of growth that is taken place during the formation of films. The typical AFM surface images (2D) of the pure and Mn doped CuI films are shown in Fig. 6.4 (a-c). A light and dark area that is found in this figure indicates greater height and friction. These predict that a strong dependence between the slope of the surface asperity and the friction co-efficient on nanometer scale. Fig. 6.5 (a,b,c) gives information about the distribution of particle size for CuI and Mn doped CuI samples. The average particle size and surface roughness of pure and Mn doped CuI films are calculated and listed in Table 6.1. The particle size and surface roughness are increased by the doping of 5 mol% Mn in CuI, while further increases of Mn doping concentration (10 mol%), the particle size and surface roughness get decreased. The possibility of bonding of oxygen atoms leading to the formation of O_2 gas and a subsequent pumping out of the gas during deposition might be the reason for the reduction in particle size. It is also reported that the oxygen gets re-evaporated from the surface at higher substrate temperatures (L. Xu et.al 2011).

Table 6.1 Grain size and Surface Roughness parameters

Sample	Grain Size (nm)	Surface Roughness (nm)
CuI	41.2	23.9
5 mol% Mn doped CuI	171	48.4
10 mol% Mn doped CuI	64.05	21.8

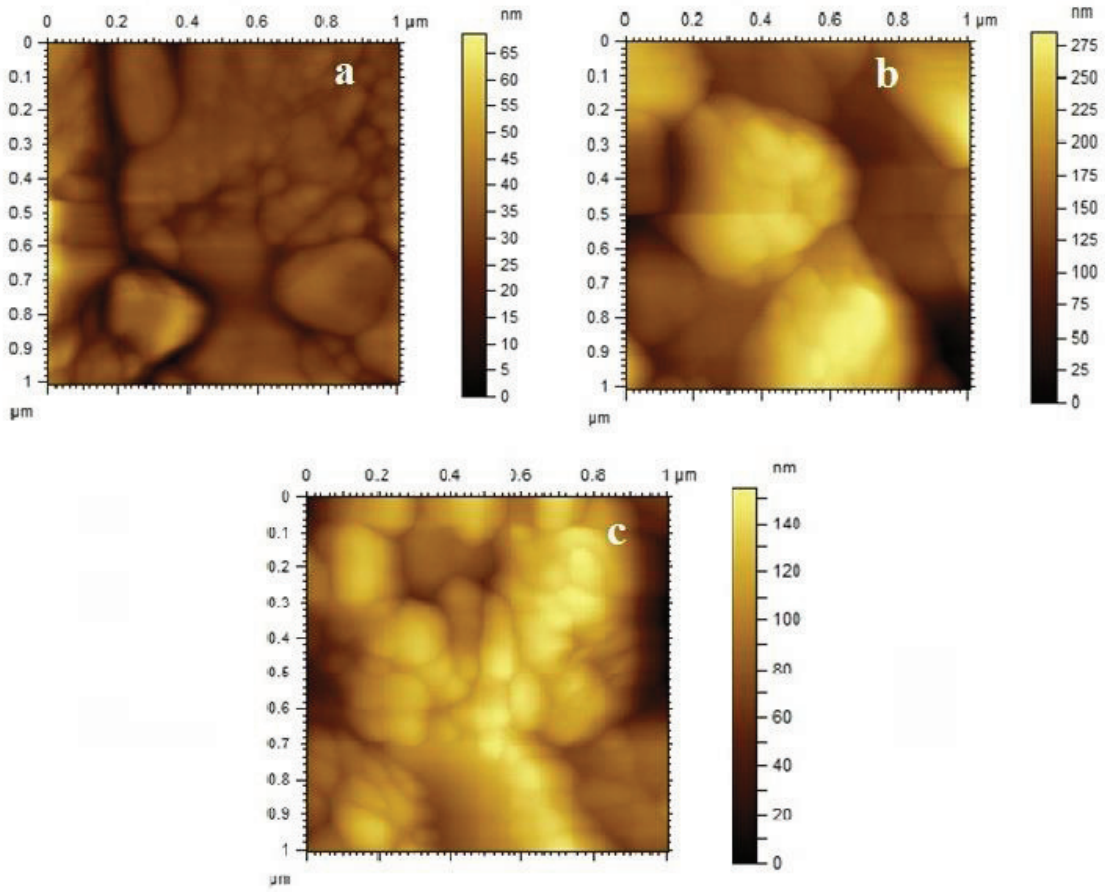

Fig 6.4(a-c) 2D AFM images of undoped and Mn doped CuI films.

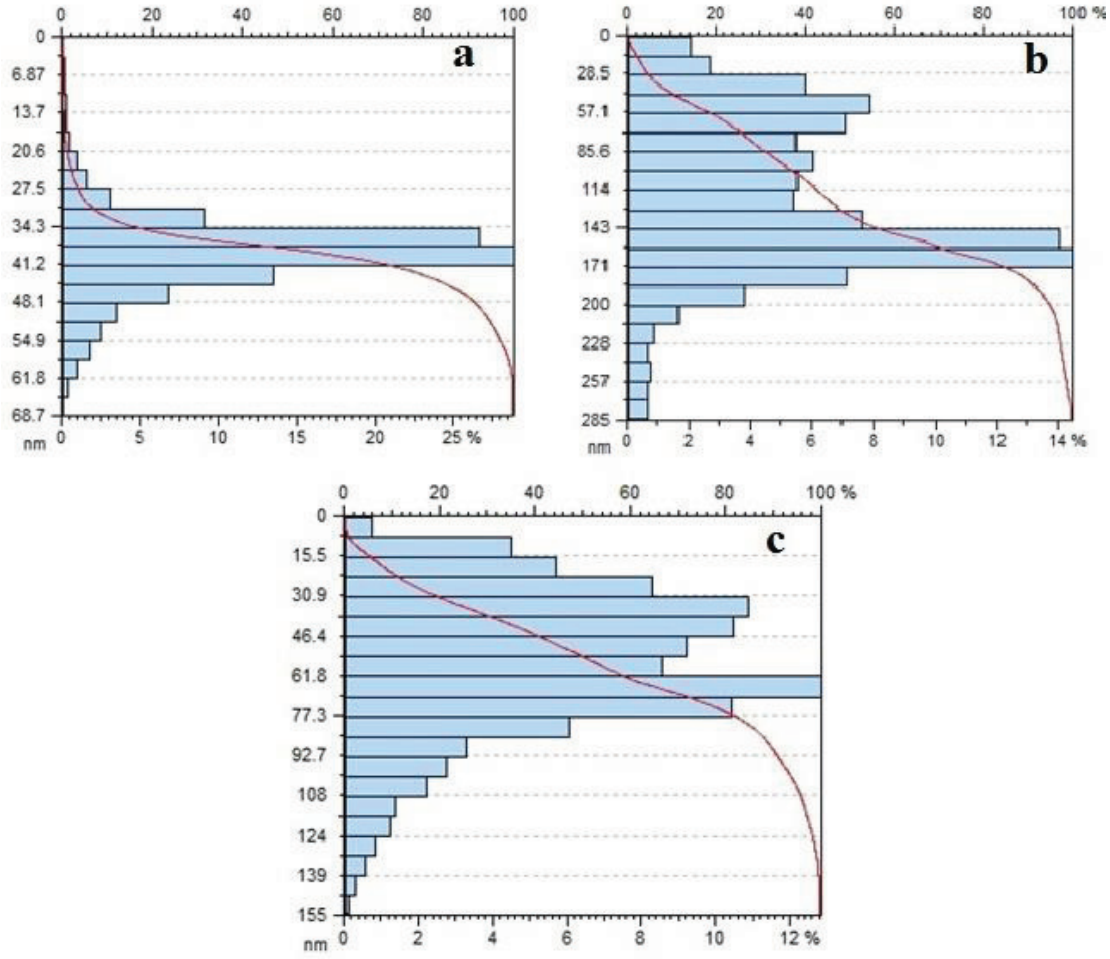

Fig 6.5(a,b,c) Particle size distribution

6.3.5 Magnetic studies

The influence of concentration of Mn atom (5 mol% and 10 mol%) on the magnetic behavior of the CuI films was studied from a plot of magnetization (M) versus applied field (H) recorded at room temperature by vibrating sample magnetometer. Figure 6.6 and 6.7exhibits the hysteresis loops of un-doped CuI and Mn doped CuI films. From Fig 6.6, it is observed that the undoped CuI sample shows diamagnetization behavior. But the doped samples (Fig 6.7) show weak ferromagnetism. From the hysteresis loops the saturation magnetization Ms of Mn doped CuI nanoparticles are found to be 0.044 emu and 0.053emu, respectively. The presence of ferromagnetism at room temperature could be attributed to the existence of sp-d exchange coupling between the local magnetic moments of Mn dopants and CuI semiconductor band electrons (T. Dietl et.al, 2000). It has also been suggested that the ferromagnetic behaviour is mediated by the formation of lattice defects in an uncontrolled manner which is induced by doping (J.M.D. Coey et.al, 2005). The inset in Fig. 6.7 shows zoomed in loop for 5 mol% Mn doped CuI film.

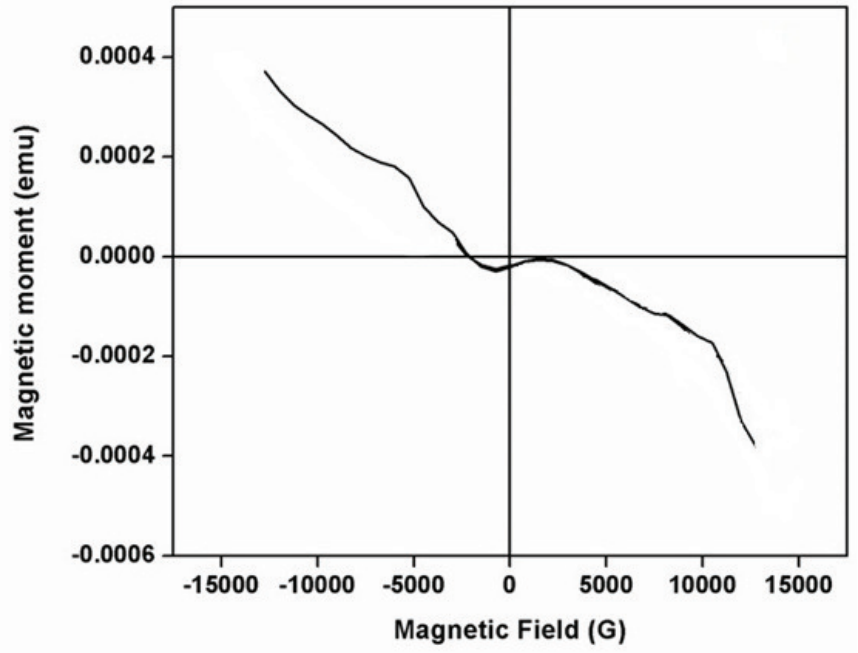

Fig 6.6 Room-temperature magnetization curve of undoped CuI film

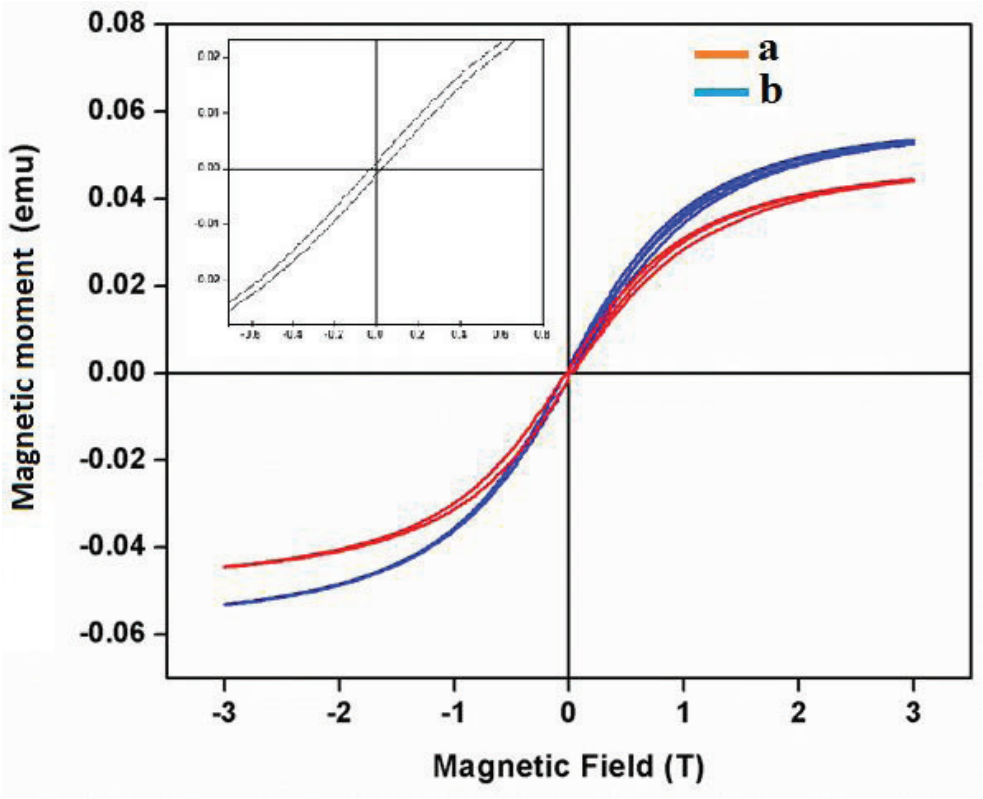

Fig 6.7 Room-temperature magnetization curves of (a) 5 mol% Mn-doped CuI (b) 10 mol% Mn-doped CuI films

6.4 Conclusion

Copper iodide and manganese doped CuI films were deposited by SILAR method. XRD pattern revealed no appreciable peak shifts among pure CuI and doped films. Increase in particle size was observed with doping concentration. UV absorption spectra of the doped CuI films revealed the shifting of the absorption edges to a region of larger wavelengths. This may be attributed to the decrease in bandgap of the films after doping. Observed decrease in bandgap with increasing Mn dopant concentration may be ascribed to the increase in particle size on doping. PL studies indicate a slight bathochromic shift and a change in the intensity of emission in the doped CuI films. From AFM studies, it is distinguished that both the particle size and surface roughness increase with respect to pure CuI in 5 mol% Mn doping while decreases in 10 mol% doping when compared 5 mol%. The reason may due to the formation of O_2 gas and subsequent pumping out. VSM results show ferromagnetic behaviour and the saturation magnetization was found to increase with the doping.